Current Biology, Volume *35*

Supplemental Information

A spinal circuit for skilled locomotion

Elisa Toscano, Nadezhda Evtushenko, Maddalena Giomi, Alessandro Santuz, Philine Thieme, Elijah David Lowenstein, Aristotelis Misios, Carmen Birchmeier, and Niccolò Zampieri

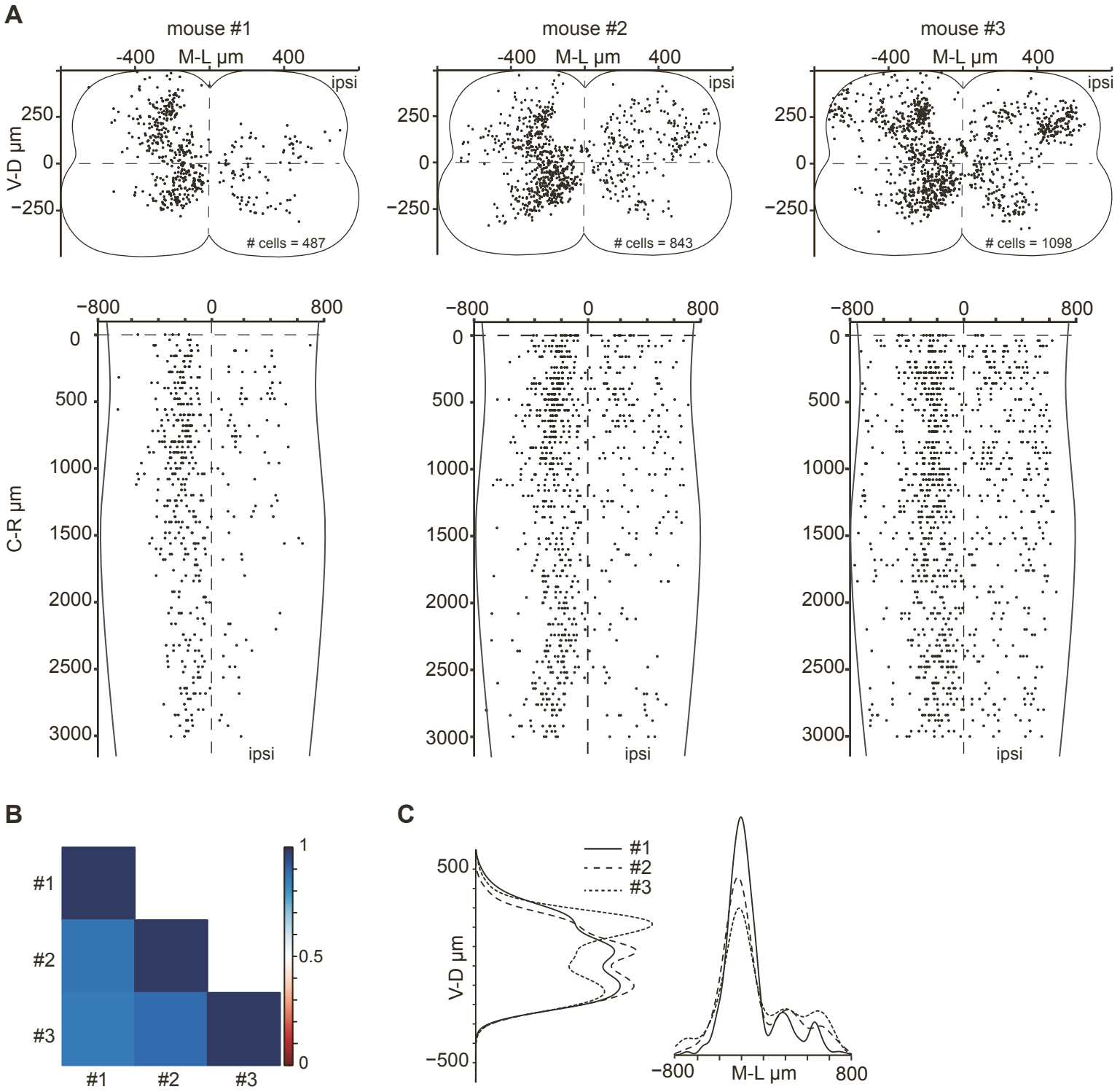

Figure S1. Anatomical characterization of long ascending neurons. Related to Figure 1.
A) Digital reconstruction of aNs position along the dorsoventral (top) and rostrocaudal (bottom) axes of the lumbar spinal cord (n = 3 mice).
B) Correlation analysis of aNs position (n = 3 mice).
C) Dorsoventral and mediolateral distribution aNs (n = 3 mice)

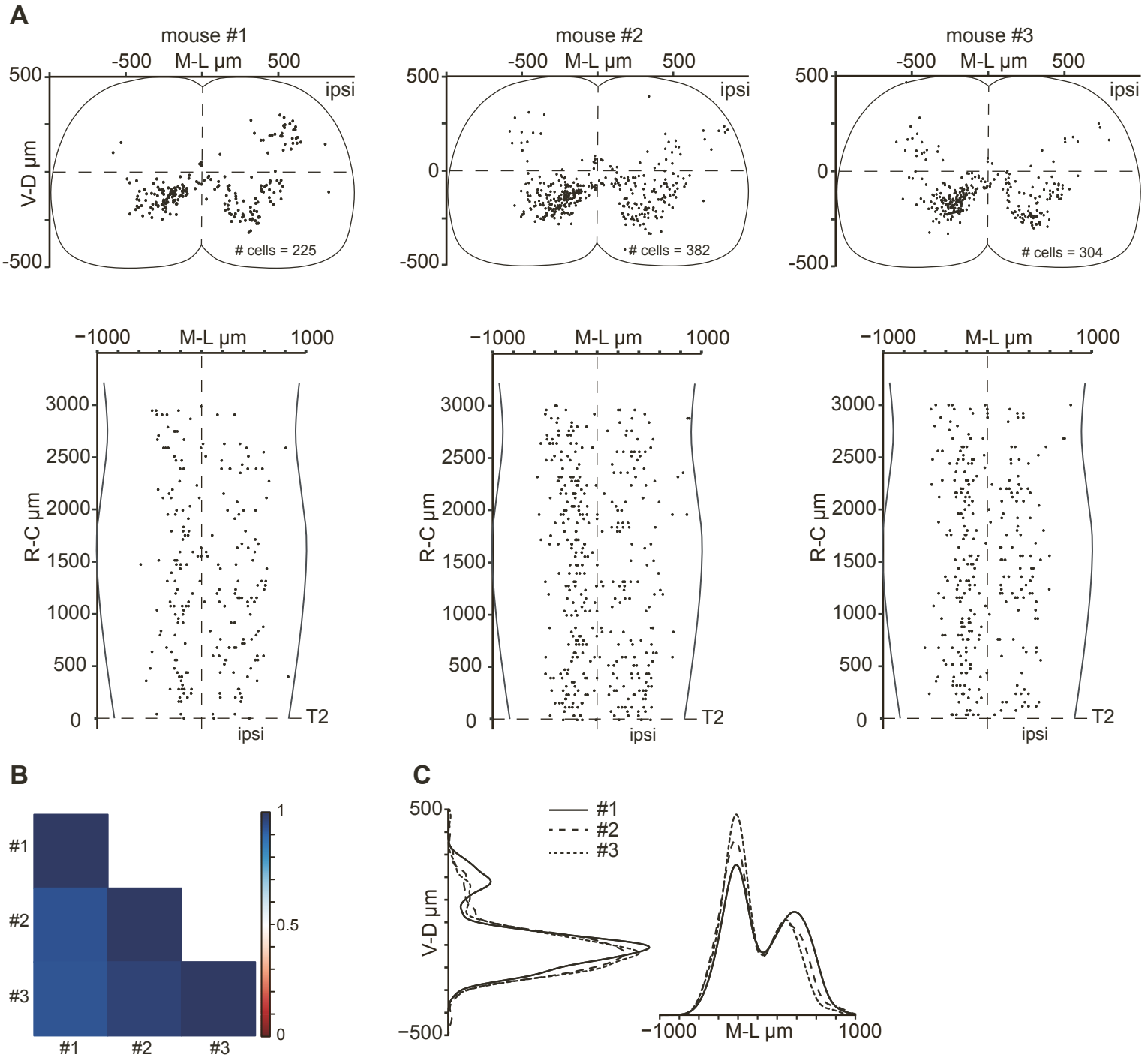

Figure S2. Anatomical characterization of long descending neurons. Related to Figure 1.
A) Digital reconstruction of dNs position along the dorsoventral (top) and rostrocaudal (bottom) axes of the cervical spinal cord (n = 3 mice).
B) Correlation analysis of dNs position (n = 3 mice).
C) Dorsoventral and mediolateral distribution dNs (n = 3 mice).

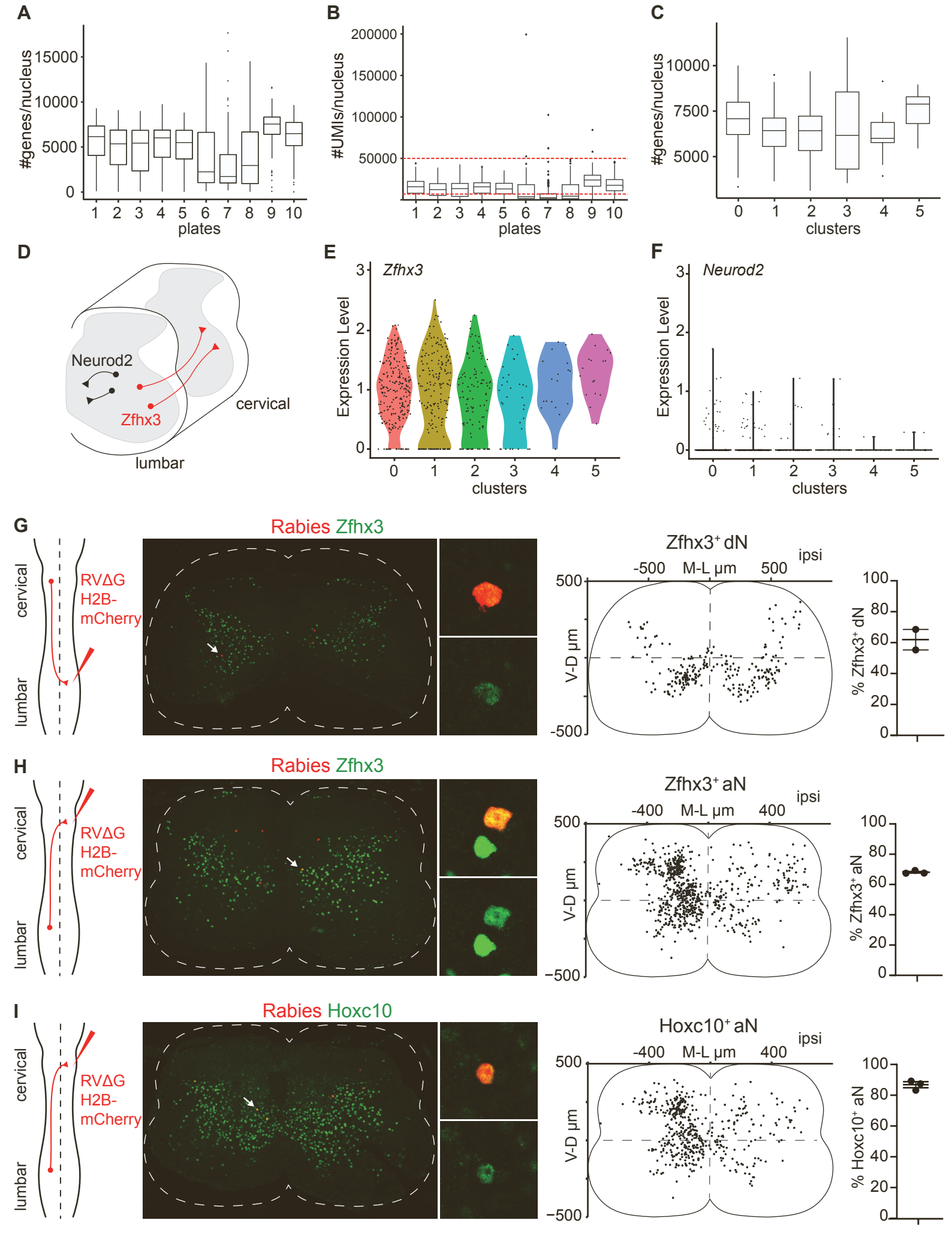
A
#genes/nucleus
15000
10000
5000
0
1 2 3 4 5 6 7 8 9 10
plates
B
#UMIs/nucleus
200000
150000
100000
50000
1 2 3 4 5 6 7 8 9 10
plates
C
#genes/nucleus
10000
7500
5000
0 1 2 3 4 5
clusters
D
Neurod2
Zfhx3
cervical
lumbar
E
Zfhx3
Expression Level
3
2
1
0
0 1 2 3 4 5
clusters
F
Neurod2
Expression Level
3
2
1
0
0 1 2 3 4 5
clusters
G
Rabies Zfhx3
cervical
lumbar
RVΔG
H2B-
mCherry
Zfhx3⁺ dN
ipsi
-500 M-L µm 500
500
V-D µm
-500
% Zfhx3⁺ dN
100
80
60
40
20
0
H
Rabies Zfhx3
cervical
lumbar
RVΔG
H2B-
mCherry
Zfhx3⁺ aN
ipsi
-400 M-L µm 400
500
V-D µm
-500
% Zfhx3⁺ aN
100
80
60
40
20
0
I
Rabies Hoxc10
cervical
lumbar
RVΔG
H2B-
mCherry
Hoxc10⁺ aN
ipsi
-400 M-L µm 400
500
V-D µm
-500
% Hoxc10⁺ aN
100
80
60
40
20
0

Figure S3. Validation of the snRNA dataset. Related to Figure 2.

A) Boxplot representing the number of genes detected per nucleus in each 96-well plate before quality control analysis. Plates #1-5 contain aNs, plates #6-10 contain dNs.

B) Boxplot representing the number of UMIs detected per nucleus in each 96-well plate before quality control analysis. The red dotted lines represent the lower (7000 UMIs) and upper (50000 UMIs) thresholds applied during quality control analysis to filter out low-quality nuclei.

C) Number of genes detected per nucleus in each cluster after quality control analysis.

D) Schematic illustrating the local and projection connectivity pattern of Neurod2+ and Zfhx3+ neurons.

E) Violin plot representing Zfhx3 expression levels in different clusters (logcounts).

F) Violin plot representing Neurod2 expression levels in different clusters (logcounts).

G) Schematic of unilateral RVΔG H2B-mCherry injection at L3-L4 used to label dNs and representative image of a cervical spinal cord showing rabies+ dNs and Zfhx3 expression. The inset shows the magnification of a representative Zfhx3+ dN. On the right: digital reconstruction of Zfhx3+ dNs position in the cervical spinal cord and percentage of Zfhx3+ dNs. (n = 2 mice, mean ± SEM).

H) Schematic of unilateral RVΔG H2B-mCherry injection at C6-C7 used to label aNs and representative image of a lumbar spinal cord showing rabies+ aNs and Zfhx3 expression. The inset shows the magnification of a representative Zfhx3+ aN. On the right: digital reconstruction of Zfhx3+ aNs position in the lumbar spinal cord and percentage of Zfhx3+ aNs. (n = 3 mice, mean ± SEM).

I) Schematic of unilateral RVΔG H2B-mCherry injection at C6-C7 used to label aNs and representative image of a lumbar spinal cord showing rabies+ aNs and Hoxc10 expression. The inset shows the magnification of a representative Hoxc10+ aN. On the right: digital reconstruction of Hoxc10+ aNs position in the lumbar spinal cord and percentage of Hoxc10+ aNs. (n = 3 mice, mean ± SEM).

.

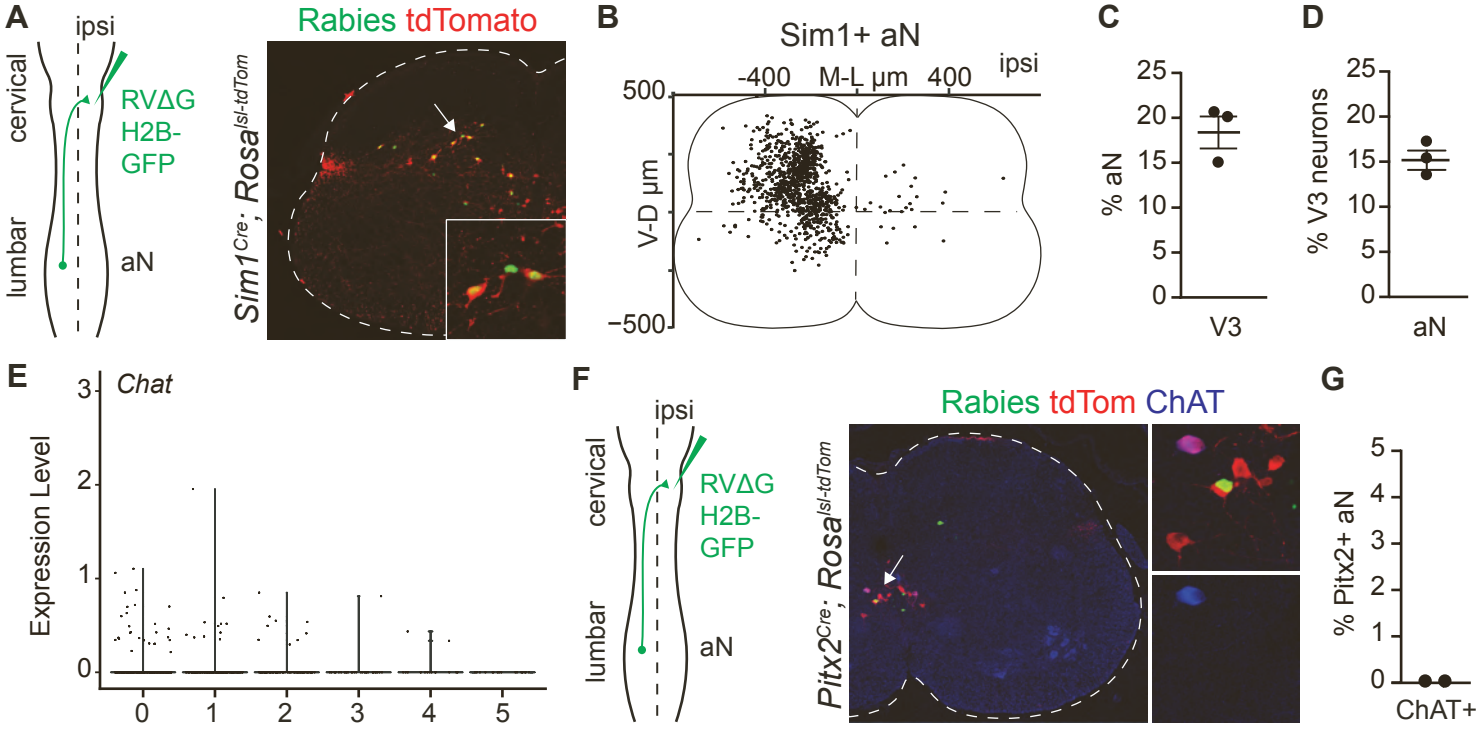

Figure S4. Validation of V3-aNs and V0-aNs. Related to Figure 3.

A) Schematic of unilateral RVΔG H2B-GFP injection at C6-C7 used to label aNs and representative image of a lumbar spinal cord showing rabies infected V3-aNs (GFP+; tdTomato+) in *Sim1*^{Cre}*; Rosa*$^{lsl\text{-}tdTomato}$ mice.
The inset shows the magnification of representative V3-aNs marked by the arrow.
B) Digital reconstruction of V3-aNs (GFP+; tdTomato+) position in the lumbar spinal cord (n = 3 mice).
C) Percentage of aNs that present V3 (tdTomato+) identity (n = 3 mice, mean ± SEM).
D) Percentage of V3 (tdTomato+) neurons that are aNs (n = 3 mice, mean ± SEM).
E) Violin plot showing *Chat* expression levels in different clusters (logcounts).
F) Schematic of unilateral RVΔG H2B-GFP injection at C6-C7 used to label aNs and representative image of a lumbar spinal cord showing rabies infected aNs (GFP+) and lineage tracing of Pitx2+ V0 (tdTomato+) neurons in *Pitx2*^{Cre}*; Rosa*$^{lsl\text{-}tdTomato}$ mice.
The inset shows the magnification of neurons marked by the arrow.
G) Percentage of Pitx2+ V0-aNs expressing ChAT (n = 2 mice).

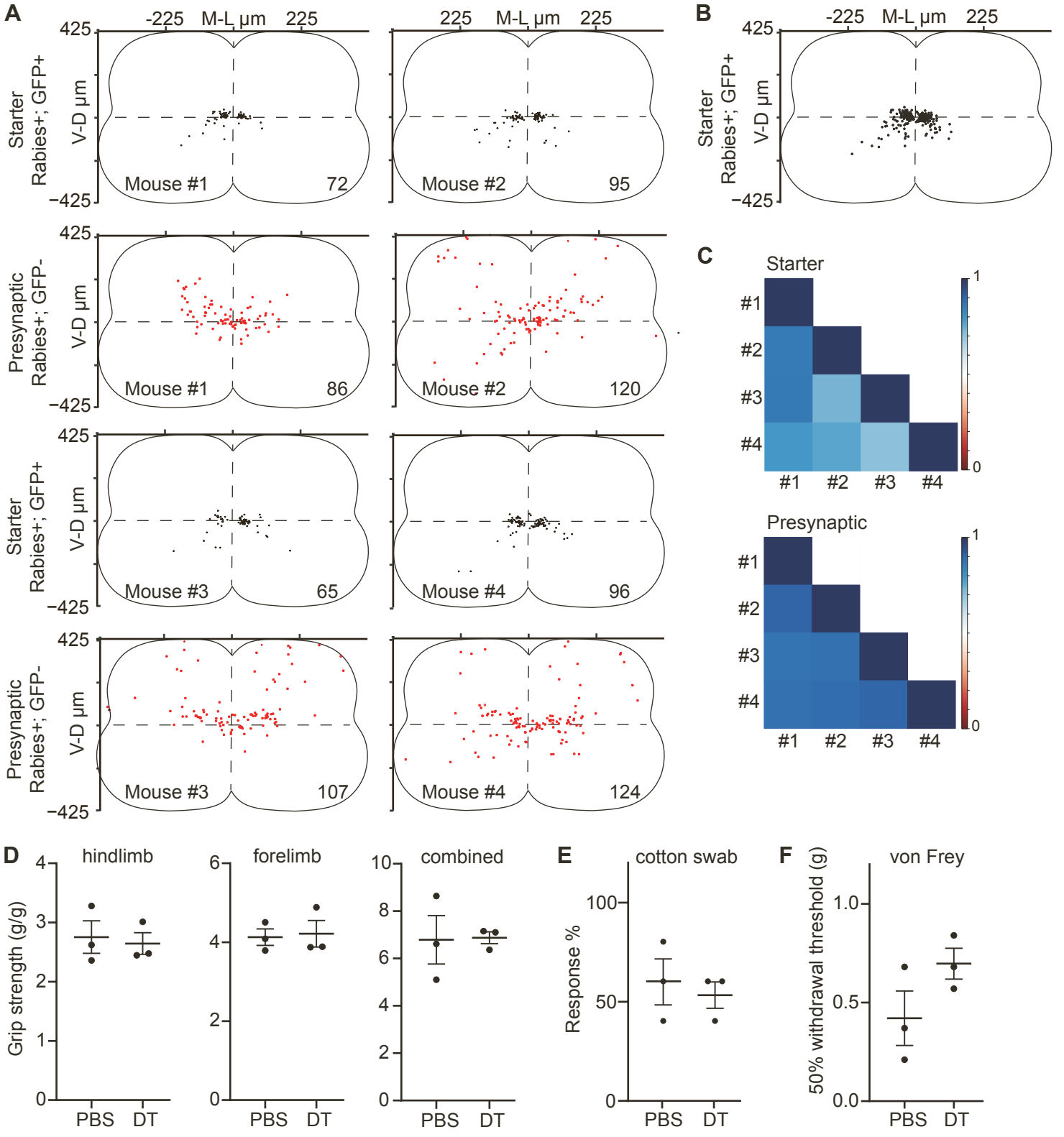

Figure S5. Anatomical and functional characterization of V0g-aNs. Related to Figure 4 and 6.

A) Starter (top, rabies+; GFP+) and presynaptic neurons (bottom, rabies+; GFP-) positions in the lumbar spinal cords of four mice. Mouse number and number of labelled neurons indicate in the bottom of each map.

B) Digital reconstruction of the position of starter cells (Rabies+; GFP+, n = 4 mice).

C) Correlation analysis of starter (top, rabies+; GFP+) and presynaptic neurons position (bottom, rabies+; GFP-). n = 4 mice.

D) \Grip strength in PBS- and DT-treated animals (n = 3 mice per group, mean ± SEM) for hindlimb (Welch's t-test p = 0.6218; middle), forelimb (Welch's t-test p = 0.5569; left), and combined (Welch's t-test p = 0.1151; right).

E) Response percentage during cotton swab test in PBS- and DT-treated animals (n = 3 mice per group, mean ± SEM; Welch's t-test p = 0.5000).

F) Withdrawal threshold during von Frey's test in PBS- and DT-treated animals (n = 3 mice per group, mean ± SEM; Welch's t-test p = 0.4881).

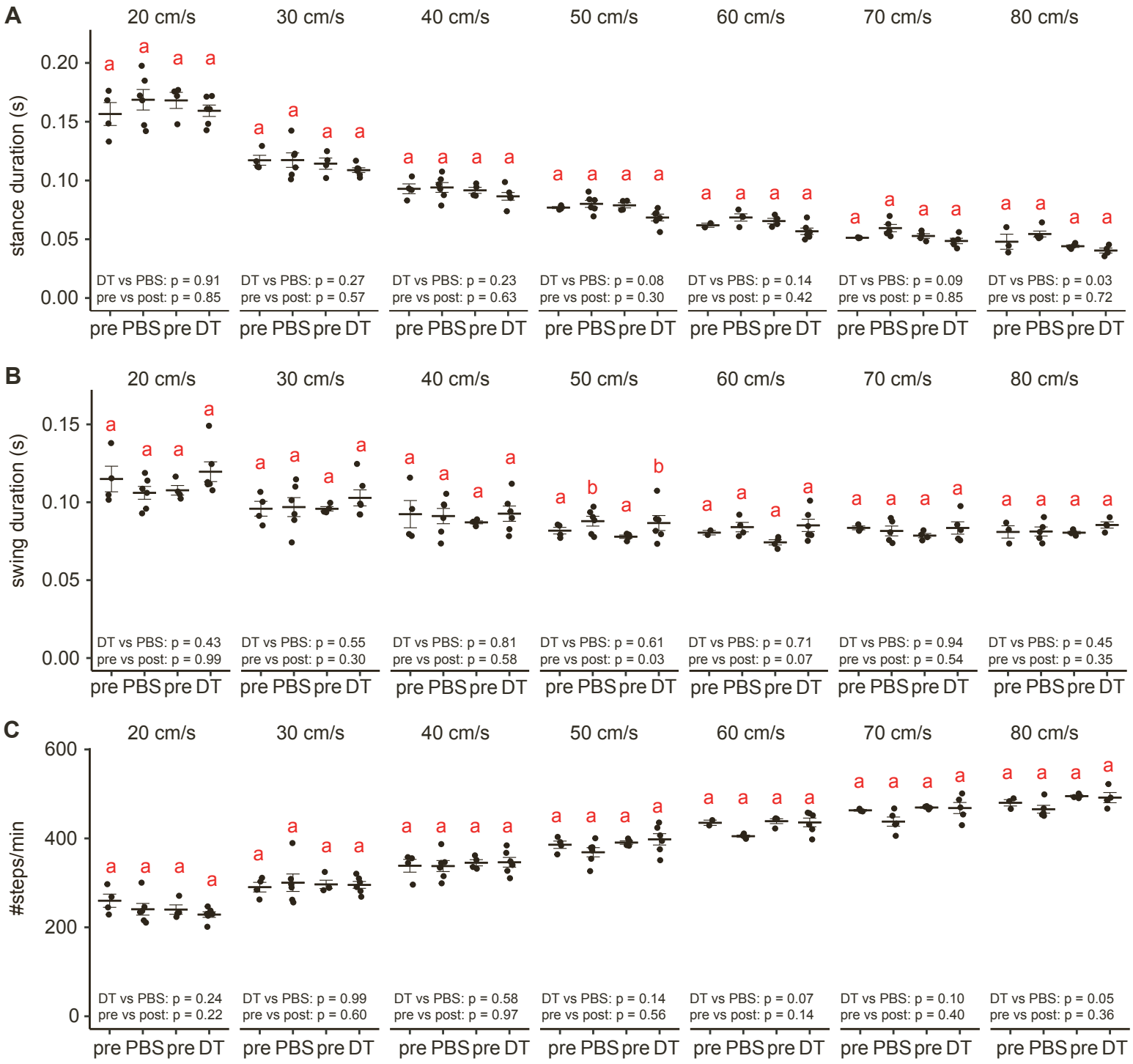

Figure S6. Elimination of V0g-aNs does not perturb kinematic parameters. Related to Figure 5.
A-C) Stance duration, B) swing duration, and C) cadence in PBS- and DT-treated mice locomoting on a treadmill at 20, 30, 40, 50, 60, 70, and 80 cm/s.
Data are mean ± SEM. The letters report the results of post-hoc pairwise comparisons.
Pairs that do not display the same letter are significantly different.

Neuron type	Descending	Descending	Descending	Ascending	Ascending	Ascending
Injection site	Lumbar	Lumbar	Lumbar	Cervical	Cervical	Cervical
Analysis site	Cervical	Cervical	Cervical	Lumbar	Lumbar	Lumbar
Mouse #	1	2	3	1	2	3
Cells/mm	75	127	101	162	281	366
# total	225	382	304	486	843	1098
# ipsi	111	157	111	94	232	368
% ipsi	49,33	41,10	36,51	19,34	27,52	33,52
# contra	114	225	193	392	611	730
% contra	50,67	58,90	63,49	80,66	72,48	66,48
# ventral	186	334	268	218	401	423
% ventral	82,67	87,43	88,16	44,86	47,57	38,52
# dorsal	39	48	36	268	442	675
% dorsal	17,33	12,57	11,84	55,14	52,43	61,48
# ipsi dorsal	33	28	13	42	159	254
% ipsi dorsal	14,67	7,33	4,28	8,64	18,86	23,13
# ipsi ventral	78	129	98	52	73	114
% ipsi ventral	34,67	33,77	32,24	10,70	8,66	10,38
# contra dorsal	6	20	23	226	283	421
% contra dorsal	2,67	5,24	7,57	46,50	33,57	38,34
# contra ventral	108	205	170	166	328	309
% contra ventral	48,00	53,66	55,92	34,16	38,91	28,14

Table S1. Number and distribution of descending and ascending neurons in rabies retrograde tracing experiments. Related to Figure 1.

1. cadence_left_forelimb
2. cadence_right_forelimb
3. cadence_left_hindlimb
4. cadence_right_hindlimb
5. stance_duration_left_forelimb
6. stance_duration_right_forelimb
7. stance_duration_left_hindlimb
8. stance_duration_right_hindlimb
9. swing_duration_left_forelimb
10. swing_duration_right_forelimb
11. swing_duration_left_hindlimb
12. swing_duration_right_hindlimb
13. cadence_sd_left_forelimb
14. cadence_sd_right_forelimb
15. cadence_sd_left_hindlimb
16. cadence_sd_right_hindlimb
17. stance_duration_sd_left_forelimb
18. stance_duration_sd_right_forelimb
19. stance_duration_sd_left_hindlimb
20. stance_duration_sd_right_hindlimb
21. swing_duration_sd_left_forelimb
22. swing_duration_sd_right_forelimb
23. swing_duration_sd_left_hindlimb
24. swing_duration_sd_right_hindlimb
25. duty_factor_left_forelimb
26. duty_factor_right_forelimb
27. duty_factor_left_hindlimb
28. duty_factor_right_hindlimb
29. phase_left_forelimb
30. phase_right_forelimb
31. phase_left_hindlimb
32. stride_length_left_forelimb
33. stride_length_right_forelimb
34. stride_length_left_hindlimb
35. stride_length_right_hindlimb
36. step_height_left_forelimb
37. step_height_right_forelimb
38. step_height_left_hindlimb
39. step_height_right_hindlimb
40. tailbase_height_right_hindlimb
41. paw_drag_left_forelimb
42. paw_drag_right_forelimb
43. paw_drag_left_hindlimb
44. paw_drag_right_hindlimb
45. ataxia_coefficient_left_forelimb
46. ataxia_coefficient_right_forelimb
47. ataxia_coefficient_left_hindlimb
48. ataxia_coefficient_right_hindlimb
49. stride_length_sd_left_forelimb
50. stride_length_sd_right_forelimb
51. stride_length_sd_left_hindlimb
52. stride_length_sd_right_hindlimb
53. step_height_sd_left_forelimb
54. step_height_sd_right_forelimb
55. step_height_sd_left_hindlimb
56. step_height_sd_right_hindlimb
57. tailbase_height_sd_left_forelimb
58. tailbase_height_sd_right_forelimb
59. tailbase_height_sd_left_hindlimb
60. tailbase_height_sd_right_hindlimb
61. paw_drag_sd_left_forelimb
62. paw_drag_sd_right_forelimb
63. paw_drag_sd_left_hindlimb
64. paw_drag_sd_right_hindlimb
65 poincare_s_hip_SD1
66. poincare_s_hip_SD2
67. poincare_s_hip_value
68. poincare_s_hip_value_emb
69. poincare_s_knee_SD1
70. poincare_s_knee_SD2
71. poincare_s_knee_value
72. poincare_s_knee_value_emb
73. poincare_s_ankle_SD1
74. poincare_s_ankle_SD2
75. poincare_s_ankle_value
76. poincare_s_ankle_value_emb
77. poincare_s_MTP_SD1
78. poincare_s_MTP_SD2
79. poincare_s_MTP_value
80. poincare_s_MTP_value_emb
81. Base_of_Support_max
82. Hip_angle_max
83. Knee_angle_max
84. Ankle_angle_max
85. MTP_angle_max
86. Base_of_Support_min
87. Hip_angle_min
88. Knee_angle_min
89. Ankle_angle_min
90. MTP_angle_min
91. Base_of_Support_rom
92. Hip_angle_rom
93. Knee_angle_rom
94. Ankle_angle_rom
95. MTP_angle_rom
96. kin_syns_HFD
97. kin_syns_Hurst
98. kin_syns_PC1
99. kin_syns_PC2
100. kin_syns_PC3

Table S2. List of kinematic parameters used for analysis of treadmill locomotion. Related to Figure 5.